

Design of a Robust Nonlinear Controller for Electric Vehicles Driven by a Six-phase Permanent-Magnet Synchronous Motor

Mohammed Kabir Bilal Boumegouas, Katia Kouzi, M'hamed Birame

Laboratory of Semiconductors and Functional Materials, Amar Telidji University of Laghouat, P. O. B. 37G, Route de Ghardaïa, Laghouat 03000, Algeria
E-mail : mk.boumegouas@lagh-univ.dz

Abstract: Electric vehicles have been a very attractive solution to resolve the atmospheric environmental pollution united by classical cars. The six-Phase Permanent-Magnet Synchronous Motor (PMSM) meets well EV the requirements, such as the high torque density and high fault tolerance. In the first stage of our study, we propose several techniques such as the IP controller as a linear control, intelligent control as a fuzzy logic control, nonlinear control such as the sliding mode control (SMC), and the integral action in SMC (ISMC). Besides the improved tracking performance with no chattering and robustness to a parametric deviation, the main SMC features, are also permissible operation states assuring an asymptotic stability of the closed-loop system. In the second stage, to check the control robustness and performance, a comparative study is made by using a dynamic model of a real EV evaluated with an NEDC driving cycle. The simulation results show that using SMC with an integral action ensures a better speed response, reduces the torque ripple and improves the durability compared to other controllers.

Keywords: electric vehicle (EV); six-phase permanent-magnet synchronous motor (PMSM); IP controller; fuzzy logic control (FLC); sliding mode control (SMC); integral action in the sliding mode (ISMC).

Zasnova robustnega nelinearnega krmilnika za šestfazni sinhroni motor s trajnimi magneti

Ko gre za uporabo obnovljivih virov energije, so električna vozila (EV) ena izmed možnosti zmanjševanja onesnaženosti ozračja. Šestfazni sinhronski motor s trajnimi magneti (PMSM) dobro izpolnjuje zahteve EV, kot sta visoka gostota navora in visoka odpornost proti napakam. V prvem koraku predlagamo več tehnoloških korakov za boljšo zmogljivost in robustnost motorja. V drugem koraku smo z uporabo dinamičnega modela EV preverili robustnost in učinkovitost krmiljenja v okviru voznega cikla NEDC. Rezultati simulacije so potrdili boljšo odzivnost, manjšo valovitost navora in izboljšano vzdržljivost motorja.

NOMENCLATURE

$V_{ds1} V_{qs1} V_{ds2} V_{qs2}$ = stator voltage in the dq frame;

$i_{ds1}, i_{ds2}, i_{qs1}, i_{qs2}$ = stator current components;

$\varphi_{abc1}, \varphi_{abc2}$ = stator flux components;

φ_r = magnet flux components;

R_s = per phase stators resistances;

$L_{d1}, L_{d2}, L_{q1}, L_{q2}$ = per phase stators leakages inductances in the dq frame;

J = inertial moment;

B = viscous friction coefficient ;

ω_e = stator pulsation;

ω_r = rotor angular speed;

T_{em} = electromagnetic torque;

T_L = load torque;

P_n = nominal power;

ISMC = integral action sliding mode

S = sliding mode surface;

k = sliding mode gain;

w_i ($i=1,2,3$) = integral action in sliding mode gain;

L_r = per phase rotor leakage inductances;

K_t = mechanical constant coefficient;

ω_s = stator pulsation;

NEDC = new european drive cycle;

P_{VE} = electric vehicle power;

F_T = total force applied on EV;

V_{VE} = EV speed;

M_{VE} = EV weight;

1 INTRODUCTION

Recently, the EV market has increased with various EV types and, is becoming more popular owing to its environmental advantages such as reduced air emissions, superior controllability and simplicity, and high efficiency. PMSMs are an attractive option meeting the EV needs, such as increased torque density, improved efficiency, maintenance-free, and small size [1,2]. Compared to traditional PMSMs, the six-phase PMSMs increase the power density and reduce the torque ripple moreover, the fault tolerance ensures the EV safety [3].

EV is a system difficult to model due to its complex physical structure composed of numerous subsystems needing a very extensive kinematic and dynamic study. The EV behavior needs a strong and robust control technique for its non-linearity and other phenomena, such as unmeasured perturbation and parameter doubts [4].

During a wide speed range, the vector control offers a great EV dynamic performance and motor operation with an optimally stable torque. The main advantages of these controllers are simplicity of realization and ease of synthesis, they are erased on classical controllers, such as PIs and PIDs, is the main deficiency, is an inadequate robustness against perturbations and parameter uncertainty.

Owing to their success the Fuzzy Logic (FLC) and Artificial Neural Network Intelligence (ANNC) controllers known as intelligent controllers, have been paid a great attention in the nonlinear systems control. This desired performance is achieved by appropriate FLC parameters. The choice of appropriate FLC parameters and their repartition in the world of static discourse includes painstaking empirical errors [8, 9].

This has resulted in a major interest in a robust and capable controller for overcoming this problem. The nonlinear control techniques have been well researched due to their superior precision, durability and simple structure assuring robust, efficient and strong design and even complex nonlinear to control high-order dynamic systems. SMC has become widely used as a powerful technique [10,12]. However, its main disadvantage is the chattering phenomenon. To solve the issue, an integral action SMC has been proposed to maintain the advantages of the ordinary SMC by eliminating the chattering phenomenon for most systems [14]. improves the precision performance adding an integral term to the control stabilizes the system enabling ISMC to improve SMC.

The focus of our work is on a six-phase PMSM drive used for EV. A mathematical model of the six-phase PMSM and field-oriented control and robust control are presented, such as the sliding mode and fuzzy logic control. An integral action in the sliding mode is developed and, its synthesis is made in six-phase PMSM. A vehicle dynamic model combined with a NEDC cycle is set up to show its suitability for EV applications.

2 A SIX-PHASE PMSM MODEL

The six-phase PMSM stator winding is shifted by thirty electrical degrees (see Fig.1). it is fed by two three-phase voltage source inverters. A Park transformation matrix is used to control the six-phase PMSM by transferring the (abc-def) winding to a synchronous rotating coordinate system.

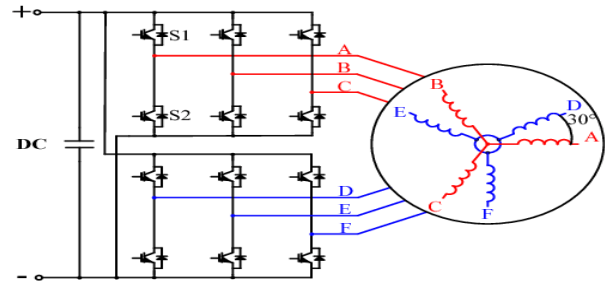


Figure 1. Configuration of the asymmetric six-phase PMSM drive.

In a three-phase system, the system of equations representing the machine is as follows:

$$\begin{aligned} V_{abc} &= R_s i_{abc1} + \frac{d}{dt}(\varphi_{abc1}) \\ V_{abc2} &= R_s i_{abc2} + \frac{d}{dt}(\varphi_{abc2}) \end{aligned} \quad (1)$$

$$\begin{aligned} \varphi_{abc1} &= L_{abc1} i_{abc1} + L_{abc1abc2} i_{abc1abc2} + \varphi_{fabc1} \\ \varphi_{abc2} &= L_{abc2} i_{abc2} + L_{abc2abc1} i_{abc2abc1} + \varphi_{fabc2} \end{aligned}$$

The model of the six-phase PMSM in the dq frame is as shows [1] and [7]:

$$\begin{aligned} \frac{d}{dt} i_{d1} &= \frac{1}{L_{d1}} [-R_s i_{d1} + \omega_e L_{q1} i_{q1} + V_{d1}] \\ \frac{d}{dt} i_{q1} &= \frac{1}{L_{q1}} [-R_s i_{q1} - \omega_e (L_{d1} i_{d1} + \varphi_f) + V_{q1}] \\ \frac{d}{dt} i_{d2} &= \frac{1}{L_{d2}} [-R_s i_{d2} + \omega_e L_{q2} i_{q2} + V_{d2}] \\ \frac{d}{dt} i_{q2} &= \frac{1}{L_{q2}} [-R_s i_{q2} - \omega_e (L_{d2} i_{d2} + \varphi_f) + V_{q2}] \end{aligned} \quad (2)$$

$$\omega_e = \frac{p}{2} \omega_r$$

The developed electromagnetic torque can be written as:

$$\begin{aligned} T_e &= \frac{3p}{2} \left([(L_{d1} i_{d1} + \varphi_f) i_{q1} + (L_{d1} - L_{q1}) i_{d1} i_{q1}] + \right. \\ &\quad \left. [(L_{d2} i_{d2} + \varphi_f) i_{q2} + (L_{d2} - L_{q2}) i_{d2} i_{q2}] \right) \end{aligned} \quad (3)$$

The six-phase PMSM mechanical dynamic equation is:

$$T_e = J \frac{d\omega_r}{dt} + B\omega_r + T_L \quad (4)$$

2.1 FOC using the IP controller

This control offers a separate control of the principal i and φ , variables for a simple model of the DC machine. The six-phase PMSM works on the basis of the vector control, $i_{d1} = i_{d2} = 0$. Hence, the torque equation is written as:

$$T_e = K_t (i_{q1} + i_{q2}) = K_t i_q^* \quad (5)$$

were

$$K_t = \frac{3p}{2} \varphi_f \quad (6)$$

In this control, the motor speed is controlled. The current controllers, using the PI controller, and the structure and synthesis of the IP and PI controller are given in [13,14].

2.2 Sliding mode control (SMC)

Compared to traditional vehicles, the EV adjustable speed is wider. The velocity is increased faster and it can be applied at high rotation states. EV therefore requires a motor at a great speed and torque [15].

To decrease chattering, the saturation function is used, to replace the discontinuous function, which determines the boundary band of the sliding surface, thus maintaining the system within the band and smoothing the control. The control law is given in [16, 17]:

$$U_n = \begin{cases} \frac{K}{\varepsilon_s} S(x) & \text{Si } |S(x)| < \varepsilon_s \\ K \text{sign}(S(x)) & \text{Si } |S(x)| > \varepsilon_s \end{cases} \quad (7)$$

2.3 Fuzzy logic control (FLC)

FLC models the uncertainty in a single-user semantic concept, i.e the uncertainty within an individual. FLC has been successfully used in machine learning as well as in controllers. FLC has two linguistic input variables: the rotational velocity error (e) and its variations (Δe) and one the linguistic output variable, i.e the electromagnetic torque variation ΔT_{em} . The T1FLC inputs equation are:

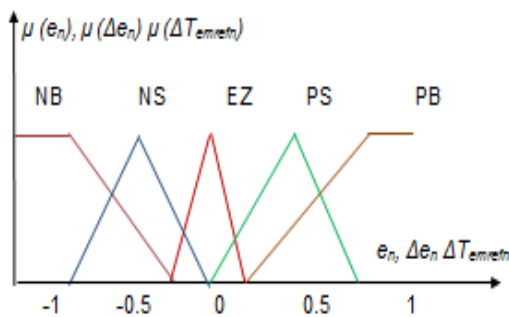
$$e(k) = K_e(\Omega_{ref}(k) - \Omega_{Dsim}(k)) \quad (8)$$

And its variation is:

$$\Delta e(k) = K_{\Delta e}(e(k) - e(k-1)) \quad (9)$$

e_n Δe_n	NB	NS	ZE	PS	PB
NB	NB	NB	NB	NS	ZE
NS	NB	NS	NS	ZE	PS
ZE	NB	NS	ZE	PS	PB
PS	NS	ZE	PS	PS	PB
PB	ZE	PS	PB	PB	PB

(a)



(b)

Figure 2. FLC Inference and membership functions, (a) table of inference rules, (b) The FLC membership functions of inputs and outputs.

The five fuzzy sets are: NB: Negative Big; NS: Negative Small; EZ: Zero; PS: Positive Small; PB: Positive Big. Hence, 25 fuzzy rules were created. the sum-product inference algorithm is used to complete the fuzzy procedure. The defuzzification process employs the gravity center method.

3 INTEGRAL ACTION SLIDING MODE CONTROL (ISMC)

ISMC, consists of an ordinary sliding surface adding an integral term to the surface (Eq.10). it completely eliminates the phase, and removes the drawbacks of the conventional SMC method by increasing and improving the transient and steady-state accuracy. This is achieved by the system trajectories on the same sliding surface. [20,23]:

$$S = e + w \int e dt \quad (10)$$

The sliding speed and current surfaces are:

$$\begin{aligned} S(\Omega) &= (\Omega - \Omega_{ref}) + w_1 \int (\Omega - \Omega_{ref}) dt \\ S(i_q) &= (i_q - i_{qref}) + w_2 \int (i_q - i_{qref}) dt \\ S(i_d) &= (i_d - i_{dref}) + w_3 \int (i_d - i_{dref}) dt \end{aligned} \quad (11)$$

Where $w_1 w_2 w_3$ Are Positive constant

3.1 ISMC Synthesis for the six-phase PMSM

In the model of the six-phase PMSM given in Eq.1, the ISMC design consists of five control loops, a velocity control loop, the two current control loops for id1 iq1 and two current control loops for id2 iq2. Since $L_d=L_q$ and R_s is a constant value, the laws of id2 iq2 the same as those of id1 iq1. Hence, the ISMC synthesis becomes a 3-loops and 2-loops design for id2 iq2.

3.1.1 Speed control loop

As shown in Eq.11, the speed control sliding surface is:

$$S(\Omega) = (\Omega - \Omega_{ref}) + w_1 \int (\Omega - \Omega_{ref}) dt \quad (12)$$

its derivative is:

$$\dot{S}(\Omega) = (\dot{\Omega} - \dot{\Omega}_{ref}) + w_1(\Omega - \Omega_{ref}) \quad (13)$$

Using the mechanical equation and its derivative, we obtain:

$$\dot{S} = -\dot{\Omega}_{ref} - \frac{3P\phi_f}{J} i_{qref} + \frac{T_L}{J} + \frac{B}{J} \Omega + w_1(\Omega - \Omega_{ref}) \quad (14)$$

with: $i_{qref} = i_q^{eq} + i_q^n$

At a sliding mode $\dot{S}(\Omega) = 0$ and $i_q^n = 0$ give:

$$I_q^{eq} = \frac{j}{\frac{3}{2}P\phi} \left(\frac{B}{J} + \frac{T_L}{J} + \dot{\Omega}_{ref} - w_1(\Omega - \Omega_{ref}) \right) \quad (15)$$

At a steady-state and convergence mode: $I_q^n = -K_{\Omega m} \text{sign}(S(\Omega))$ (16)

where w_1 and $K_{\Omega m}$ are a real positive.

3.1.2 Current i_{q1} control loop

The sliding surface for the current iq1 control is:

$$S(i_q) = (i_q - i_{qref}) + w_3 \int (i_q - i_{qref}) dt \quad (17)$$

Its derivative is:

$$\dot{S}(i_q) = (i_q - i_{qref}) + w_1(i_q - i_{qref}) \quad (18)$$

Using Eq.2 gives:

$$\dot{S} = -\frac{R_s}{L_{q1}} i_{q1} - (L_{d1} i_{d1} + \varphi_f) \frac{\omega_r}{L_{q1}} + \frac{1}{L_{q1}} V_{q1ref} - i_{q1ref} + w_2(i_{q1} - i_{q1ref}) \quad (19)$$

$$\text{and: } V_{q1ref} = V_{q1}^{eq} + V_{q1}^n$$

At the sliding mode $\dot{S}(i_q) = 0$ and $V_{q1}^n = 0$:

$$V_{q1}^{eq} = L_{q1} \left[\frac{R_s}{L_{q1}} i_{d1} + \frac{\omega_r L_{d1}}{L_{q1}} i_{d1} + \frac{\omega_r \varphi_f}{L_{q1}} + i_{q1ref} - w_2(i_{d1} - i_{d1ref}) \right] \quad (20)$$

At a steady-state and convergence mode:

$$V_{q1}^n = -K_{q1} \text{sign}(S(i_q)) \quad (21)$$

where w_2 and K_{iq1} is a real positive.

3.1.3 Current i_{d1} control loop

The sliding surface for the current i_{d1} control is:

$$S(i_d) = (i_d - i_{dref}) + w_2 \int (i_d - i_{dref}) dt \quad (22)$$

and its derivative:

$$\dot{S}(i_d) = (i_d - i_{dref}) + w_1(i_d - i_{dref}) \quad (23)$$

Using the first equation in Eq.2, we get:

$$\dot{S} = -\frac{R_s}{L_{d1}} i_{d1} + \frac{\omega_r L_{q1}}{L_{d1}} i_{q1} + \frac{1}{L_{d1}} V_{d1eq} - i_{d1ref} + w_2(i_{d1} - i_{d1ref}) \quad (24)$$

$$\text{with } V_{d1ref} = V_{d1}^{eq} + V_{d1}^n$$

At the sliding mode $\dot{S}(i_d) = 0$ and $i_d^n = 0$:

$$V_{d1}^{eq} = L_{d1} \left[\frac{R_s}{L_{d1}} i_{d1} - \frac{\omega_r L_{q1}}{L_{d1}} i_{q1} + i_{d1ref} - w_2(i_{d1} - i_{d1ref}) \right] \quad (25)$$

At the steady-state and convergence mode:

$$V_{d1}^n = -K_{d1} \text{sign}(S(i_d)) \quad (26)$$

where w_3 and K_{id1} is a real positive.

4 EV APPLICATION

EV model is used to check the dynamic performance of the presented control.

4.1 Dynamic EV model

The used EV model of an urban type. Resistive forces oppose EV advancement. The forces effecting EV are shown in Fig. 3:

The system of equations representing the EV dynamic model using the evaluation of the NEDC cycle is:

$$P_{VE} = F_T V_{VE} = (F_{roue} + F_{pente} + F_{aero} + F_{acc}) V_{VE} \quad (26)$$

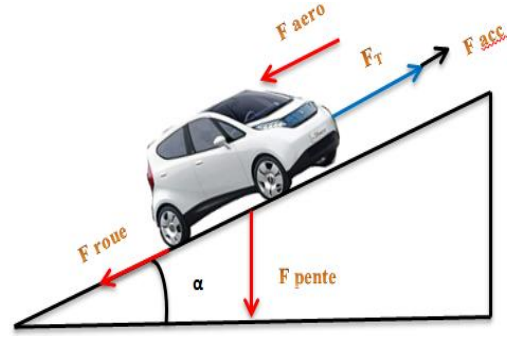


Figure 3. Forces effecting EV.

$$P_{VE} = (M_{VE} \cdot g \cdot (C_0 + C_1) \cdot V_{VE}^2 + M_{VE} \cdot g \cdot \sin \alpha + 0.5 \cdot \rho \cdot C_x \cdot V_{VE}^2 + M_{VE} \cdot r \cdot \frac{d\Omega_{roue}}{dt}) V_{VE} \quad (27)$$

Table .1 shows the EV parameters [24].

Table 1. EV characteristics.

EV Parameter	Value
EV weight	820 kg
Force of gravity	9.81 m/s2
Wheel Radius	0.33 m
Air Density	1.2 kg/m3
Front surface(S)	2.75
Air penetration coefficient (Cx)	0.3
Rolling resistance coefficient in a dynamic state (C0)	1.6e-6
Rolling resistance coefficient in a Static State (C1)	0.008
Road slope (α)	2.5%

The NEDC driving cycle is used to describe the route and to reproduce the real EV states [25].

Fig 4. Shows a global EV ISMC synoptic diagram for PMSM.

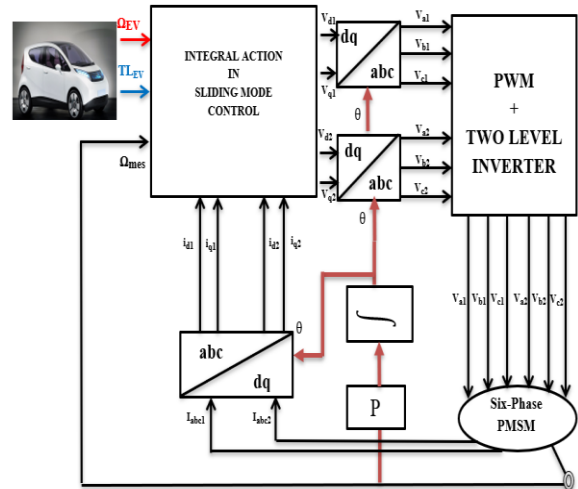


Figure 4. EV ISMC Global diagram for PMSM.

5 SIMULATION RESULTS

Simulations performed MATLAB/Simulink confirm the advantages provided by the presented controller, table 2 represents the motor characteristics

Table 2. Six-phase PMSM parameters.

Six-phase PMSM Parameters	Values
R_s	1.9 Ω
L_d	8.35e-4 H
L_q	8.35e-4 H
P	4
J	0.015 KG.M ²
B	2.5 N.M.S/RD
φ	0.353 Wb
V dc	800 V
Nominal power	12 KW
Nominal speed	100 rad/s
Nominal torque	120 N.m

Table 3. The controllers gain values.

Contr ollers	IP	SMOOTH H	FUZZY	ISMC
i_d	$K_p=19$ $K_i=4.3234e^3$	$K_d=178$ $\varepsilon_d=0.01$	//	$K_d=178$ $w_3=0.01$
i_q	$K_p=19$ $K_i=4.3234e^3$	$K_q=650$ $\varepsilon_q=0.01$	//	$K_q=178$ $w_2=0.01$
Speed Ω	$K_p=10.8661$ $K_i=2.0026e^3$	$K_m=176$ $\varepsilon_m=0.25$	$K_e=800$ $\Delta K_e=0.05$	$K_m=178$ $w_1=0.01$

To assess the performance and robustness of the presented controllers, a comparison is made between

Table 4. Performance of the various controllers.

Controller	Response time at a reference speed	Overshoot Pic (rad/s)	Torque ripple	Perturbation reject at nominal TL
IP	0.021 s	0	5.81%	0.025 s
FUZZY	7.6 ms	100.348	6.6 %	3.4 ms
SMC	4.6 ms	100.183	5.8 %	0.2 ms
ISMC	4.45 ms	100.5	5.9 %	0.46 ms

their various type, such as the IP, SMC, FLC, SMC controller with an integral action. Table 3 shows their gain values.

In as simulations, the reference speed is 50 rad/s and 100 Rad/s at 0.5s. The load torques, is 30N.m and 120N.m at 0.7s.

The results show that the SMC is powerful robustness, and its performance is high compared to the IP control (see Figure 5). The SMC controller, outperforms the IP controller in terms of its dynamic performance, disturbance rejection resistance, and accuracy. Figure 6 shows that both SMC with and integral action and FLC provide a high performance and robustness in term of the speed and torque. Besides SMC with the Integral action gives fewer peaks at a load variation.

As seen from Table 4, all the controllers show a good performance. Nevertheless, ISMC outperforms the others in terms of its perturbation resistance, and response time.

To check the effectiveness of the proposed controller, a comparison is made between IP, SMC, FLC and SMC with an integral action, and a dynamic model of a real EV evaluated by the NEDC driving cycle.

The results given in Figures 8 and 9 show that the six-phase PMSM follows the quantities of the EV commands. As shown in Fig.9, in SMC there are a considerable error and ripple in the acceleration and deceleration phase which limit the dynamic performance. In SMC with an integral action there are small peaks in the acceleration and deceleration phase compared to SMC (see Fig.8) which may affect the vehicle. Figs .8,c and .9,c show that the power supplied by the electric drive follows well the power demanded by EV. In the acceleration and deceleration mode, the dynamic errors are small, and the losses with the integral action are fewer compared to when using the SMC controller.

The EV traction chain is improved by the fast perturbation rejection and reduced torque ripple when using the ISMC controller, the THD results are given in Table ,5 and Fig 9.

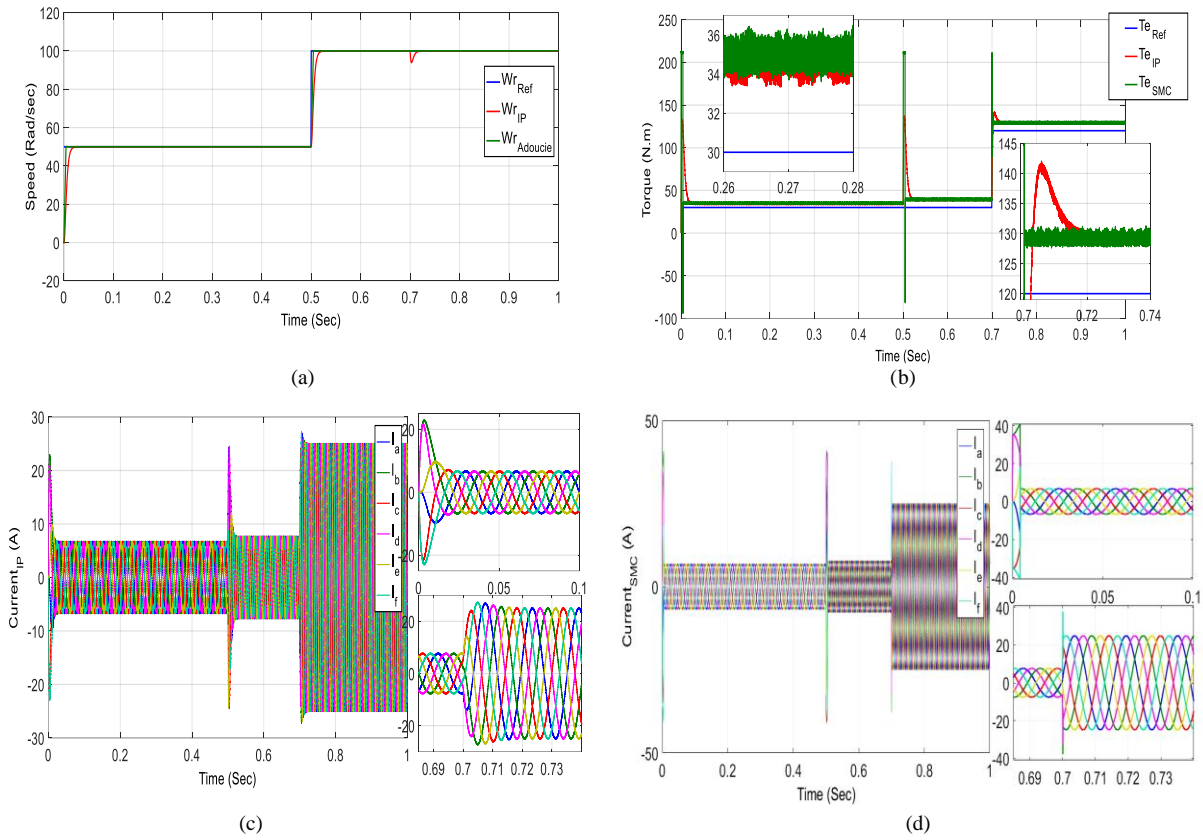


Figure 5. PI and SMC simulation results for a six-phase PMSM, (a) Speed performance; (b) Torque response; (c) PI stator currents; (d) SMC stator currents.

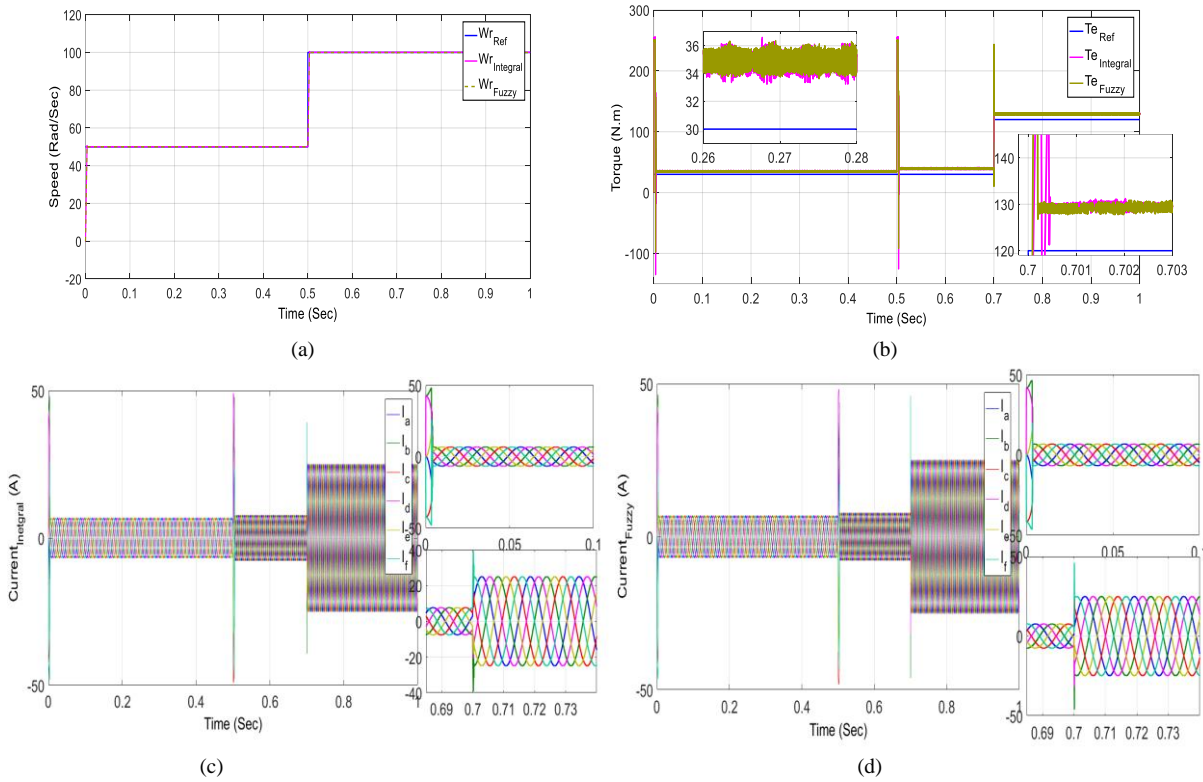


Figure 6. FLC and ISMC simulation results for a six-phase PMSM, (a) Speed performance; (b) Torque response; (c) PI stator currents; (d) SMC stator currents.

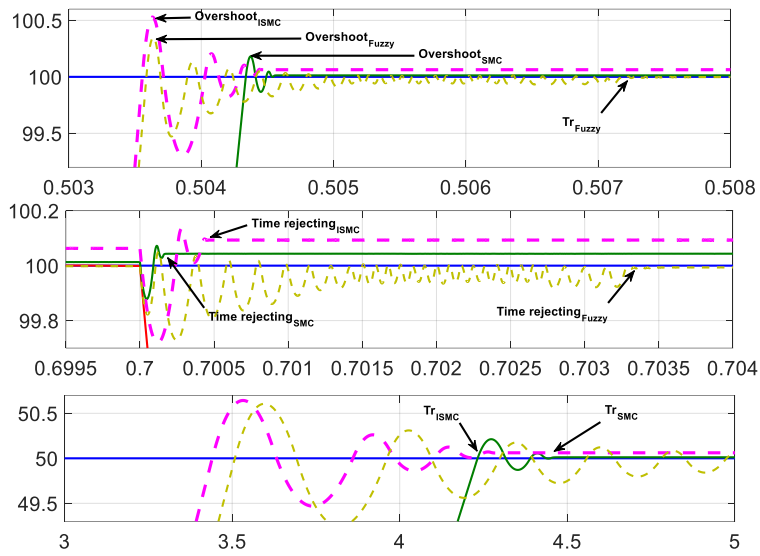


Figure 7. Speed values for various controllers at the same operating states.

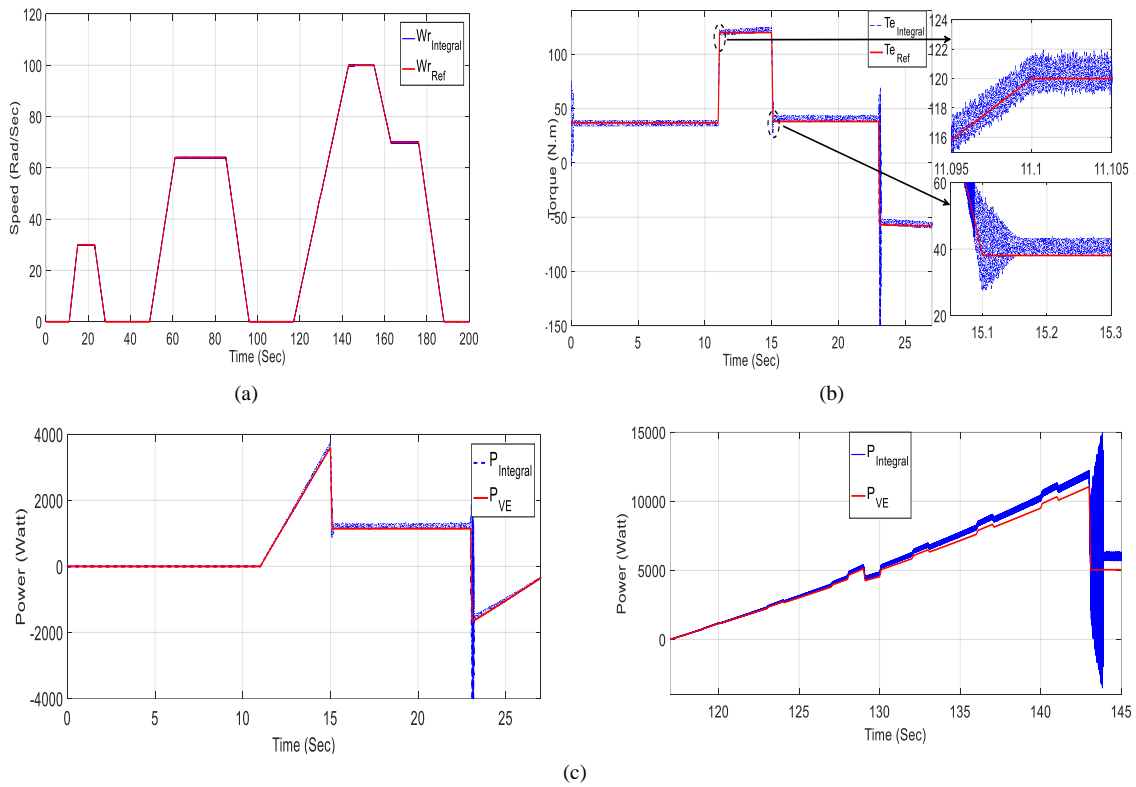


Figure 8. Simulation results of application of the integral action in the SMC controller on EV, (a) Speed performance. (b) Torque response. (c) Power response.

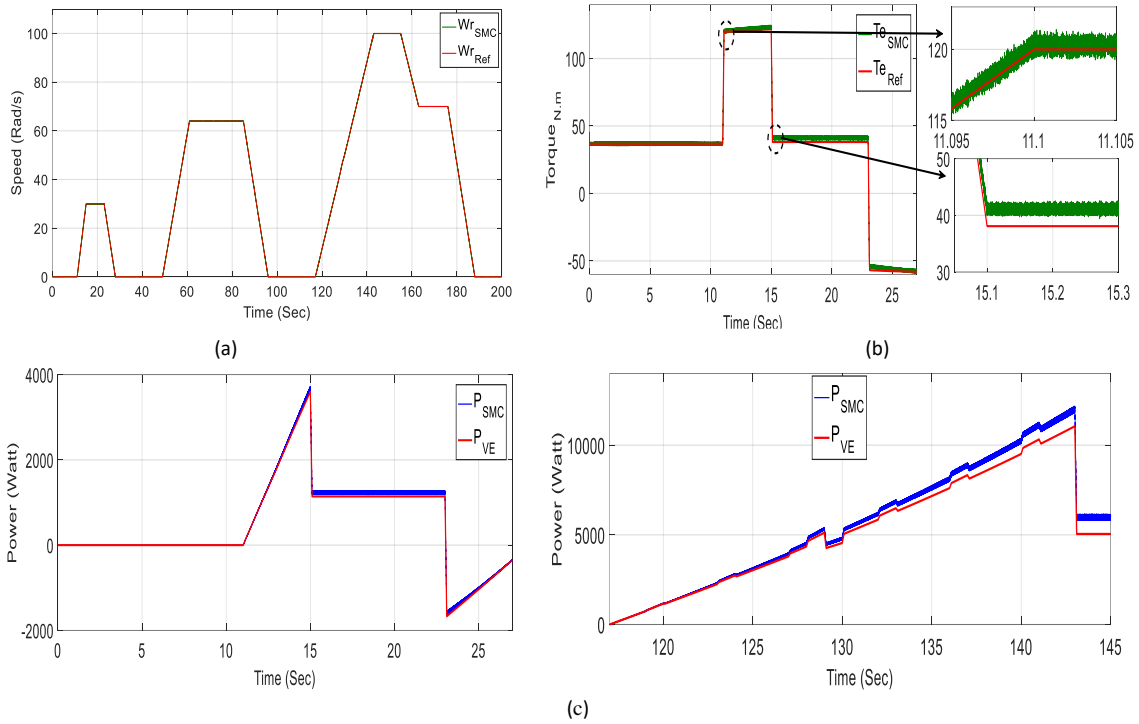


Figure 9. Simulation results of application of SMC on EV, (a) Speed performance. (b) Torque response. (c) Power response.

Table 5. THD analysis results for the integral action sliding-mode control.

	ISMC
Torque	91.81%
Quadrature current	91.84%

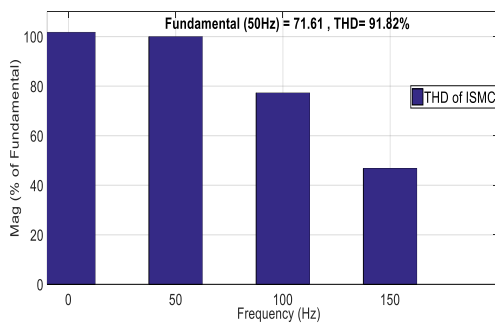


Figure 10. FFT analysis of the electromagnetic torque for ISMC.

6 CONCLUSION

The paper proposes several non-linear controls to improve the performance and durability of the EV traction chain of a six-phase PMSM. Besides improving the tracking performance with no

chattering and robustness to parametric deviation, the proposed ISMC ensures an asymptotic stability of the closed-loop system during permissible operating states, and is easy to implemented.

The experimental results show that the proposed controller outperforms other nonlinear controllers in terms of the chattering phenomenon issue, response, and robustness against external perturbation.

In our future work, the EV chain will be completed, an advanced battery will be used to ensure a long autonomy and a novel control algorithm of the DC-DC converter will be applied. Some control technique to improve the velocity and electromagnetic, and load torque will be further estimated by using a robust observer, such as the algebraic and sliding mode observer. The proposed controller will be implemented in a real system.

REFERENCES

- [1] Pan, C., Gu, X., Chen, L., Chen, L. and Yi, F., Driving cycle construction and combined driving cycle prediction for fuzzy energy management of electric vehicles. *International Journal of Energy Research*, 45(12), str.17094-17108, 2021.
- [2] Kittner, N., Tsiropoulos, I., Tarvydas, D., Schmidt, O., Staffell, I. and Kammen, D.M., Electric vehicles. In *Technological Learning in the Transition to a Low-Carbon Energy System* (str. 145-163). Academic Press, 2020.
- [3] Benariba, H. and Boumediène, A., Super twisting sliding mode control of an electric vehicle. In *2015 3rd International Conference on Control, Engineering & Information Technology (CEIT)* (str. 1-6). IEEE, May, 2015.

- [4] Sant, A.V., Khadkikar, V., Xiao, W. and Zeineldin, H.H., Four-axis vector-controlled dual-rotor PMSM for plug-in electric vehicles. *IEEE Transactions on Industrial Electronics*, 62(5), str. 3202-3212. 2014.
- [5] Lara, J., Xu, J., & Chandra, A. Effects of rotor position error in the performance of field-oriented-controlled PMSM drives for electric vehicle traction applications. *IEEE Transactions on Industrial electronics*, 63(8), str.4738-4751. 2016.
- [6] Tong, C., Wu, F., Zheng, P., Sui, Y., & Cheng, L. Analysis and design of a fault-tolerant six-phase permanent-magnet synchronous machine for electric vehicles. In 2014 17th International Conference on Electrical Machines and Systems (ICEMS) (str. 1629-1632). IEEE, October, 2014.
- [7] Bekiroglu, E., & Dalkin, A. Comparison of Trapezoidal and Sinusoidal PWM Techniques for Speed and Position Control of PMSM. *Advances in Electrical and Electronic Engineering*, 18(4), str.207-216. 2020.
- [8] Kouzi, K., & Naït-Saïd, M. S. Adaptive fuzzy logic speed-sensorless control improvement of induction motor for standstill and low speed operations. *COMPEL-The international journal for computation and mathematics in electrical and electronic engineering*. 2007.
- [9] Kouzi, L. M. K. Influence of fuzzy adapted scaling factors on the performance of a Fuzzy logic controller based on an indirect vector control for induction motor drive. *Journal of Electrical Engineering*, 55(7-8), str. 188-194. 2004.
- [10] Utkin, V. Variable structure systems with sliding modes. *IEEE Transactions on Automatic control*, 22(2), str. 212-222. 1977.
- [11] Bartolini, G., Fridman, L., Pisano, A., & Usai, E. (Eds.). *Modern sliding mode control theory: New perspectives and applications* (Vol. 375). Springer Science & Business Media. 2008.
- [12] Utkin, V., Guldner, J., & Shi, J. *Sliding mode control in electro-mechanical systems*. CRC press. 2017.
- [13] Bris, P., Vittek, J., & Makys, P. Position Control of PMSM in Sliding Mode. *Advances in Electrical and Electronic Engineering*, 7(1-2), str. 198-201. 2011.
- [14] Bounasla, N., & Hemsas, K. E. Second order sliding mode control of a permanent magnet synchronous motor. In 14th international conference on Sciences and Techniques of Automatic control & computer engineering-STA'2013 (str. 535-539). IEEE, December, 2013.
- [15] Hung, Y. C., & Lin, F. J. 2013. Intelligent Fault Tolerant Control of Six-Phase Permanent Magnet Synchronous Motor Drive System for Light Electric Vehicle. Available at: <http://www.ee.ncu.edu.tw/~linfj/PDF/Intelligent20Fault%20olerant%20Control%20of%20SixPhase20Permanent%20Mag net%20Synchronous%20Motor.pdf>.
- [16] RAZAFINJAKA, J. N., & Patrick, A. T. COMPARAISON DES PERFORMANCES DES REGULATEURS PI ET IP APPLIQUES AUX SYSTEMES FONDAMENTAUX. Researchgate Inc., 2015, online: https://www.researchgate.net/publication/272748849_COMP ARAISON DES PERFORMANCES DES REGULATEUR S_PI_ET_IP_APPLIQUES_AUX_SYSTEMES_FONDAME NTAUX (29.12.2020)
- [17] Lokriti, A., Zidani, Y., & Doubabi, S. Comparaison des performances des régulateurs PI et IP appliqués pour la commande vectorielle à flux rotorique orienté d'une machine asynchrone. In 8ème Conférence Internationale de MOdélisation et SIMulation-MOSIM'10. Tunisie, May, 2010. online: https://www.researchgate.net/publication/259182062_COMPARAI SON DES PERFORMANCES DES REGULATEURS PI ET_IP_APPLIQUES_POUR_LA_COMMANDE_VECTORI ELLE_A_FLUX_ROTORIQUE_ORIENTE_D'UNE MACHI NE_ASYNCHRONE (30.12.2020).
- [18] Haoyu, Z., Gang, Y., Lidan, Z., Boshan, M., & Dongdong, L. Sliding mode control based on six-phase PMSM speed control system. In IECON 2017-43rd Annual Conference of the IEEE Industrial Electronics Society (str. 8819-8824). IEEE. 2017.
- [19] Larbaoui, A., Belabbes, B., Meroufel, A., & Bouguenna, D. FUZZY SLIDING MODE CONTROL FOR SYNCHRONOUS MACHINE. *REVUE ROUMAINE DES SCIENCES TECHNIQUES-SERIE ELECTROTECHNIQUE ET ENERGETIQUE*, 62(2), str.192-196. 2017.
- [20] Bahi, T., Lachtar, S., Soufi, Y., Lekhchine, S., & Merabet, H. Speed control by sliding mode of synchronous motor. In International Aegean Conference on Electrical Machines and Power Electronics and Electromotion, Joint Conference (str. 386-391). IEEE, September, 2011.
- [21] Utkin, V., & Shi, J. Integral sliding mode in systems operating under uncertainty conditions. In Proceedings of 35th IEEE conference on decision and control (Vol. 4, str. 4591-4596). IEEE, December, 1996.
- [22] Templos-Santos, J. L., Aguilar-Mejia, O., Beltran-Carbajal, F., Valderabano-Gonzalez, A., & Tapia-Olvera, R. Integral Action in Sliding Mode Control for Reduction of Chattering in Speed Regulation of a Synchronous Motor. In *Journal of Physics: Conference Series* (Vol. 1221, No. 1, str. 012060). IOP Publishing, June, 2019.
- [23] Barlow, T. J., Latham, S., McCrae, I. S., & Boulter, P. G. A reference book of driving cycles for use in the measurement of road vehicle emissions. TRL Published Project Report. 2009. online: https://assets.publishing.service.gov.uk/government/uploads/system/uploads/attachment_data/file/4247/ppr-354.pdf (29.12.2020)
- [24] Bendjedia B, Bouchafaa F, Rizoug N, Boukhniher M. Comparative study between battery and supercapacitor hybridization with fuel cells for automotive applications. 4th Int. Conf. Control. Decis. Inf. Technol. CoDIT 2017, vol. 2017-January, pp. 833-838. 2017.
- [25] Xu, X., Dong, P., Liu, Y., & Zhang, H. Progress in automotive transmission technology. *Automotive Innovation*, 1(3), str.187-210. 2018.

Mohammed Kabir Bilal Boumegouas received his M.Sc. degree from the Amar Telidji University of Laghouat, Algeria, in 2019. Currently, he is a Ph.D. student at the same University. His research interests are in advanced control of the electric vehicle, sensorless control, intelligent artificial control, and electric vehicle storage system.

Katia Kouzi received her Engineer and Master degrees in Electrical Engineering in 1998 and 2002, respectively, and her Ph.D. degree in Electrical and Computer Engineering in 2008 from University of Batna, Algeria. Her research interests are in advanced control of ac drives, including vector, sensorless, intelligent artificial control, electric vehicles (EVs) control, and renewable energy systems control, managements and storage systems. She is a researcher with the semi-conductors and Functional Materials Laboratory, and a full professor at the Electrical Engineering Institute at the Laghouat University, Algeria.

M'hamed Birame received his Master and Ph.D. degrees in Power Electronics in 2005 and 2015 respectively. Since 2005 he has been an assistant Professor with the Electrical Engineering Department of the Laghouat University, Algeria. His main research area includes modeling of electrical machines, electric drives control, and power electronics.